

Decoherence of quantum superpositions through coupling to engineered reservoirs*

C.J. Myatt, B.E. King, Q.A. Turchette, C.A. Sackett, D. Kielpinski,
W.M. Itano, C. Monroe, and D.J. Wineland

Time and Frequency Division, National Institute of Standards and Technology, Boulder, Colorado 80303

The theory of quantum mechanics applies to closed systems. In such ideal situations, a single atom can exist, for example, in a superposition of being in two different positions at the same time. In contrast, real systems always interact with their environment, with the consequence that macroscopic quantum superpositions like Schrödinger's cat are not observed. Moreover, macroscopic superpositions decay so quickly that the dynamics of decoherence may not even be observed. However, mesoscopic systems offer the possibility of observing the decoherence of such quantum superpositions. Here we present measurements of decoherence of superposition states of the motion of a single trapped atom. Decoherence is induced by coupling the atom to *engineered* reservoirs, where the coupling and state of the environment are under the experimenter's control. We exhibit this with three experiments, finding that the decoherence scales exponentially with the square of the size of the superposition.

One of the fundamental properties of quantum mechanics is the principle of superposition, a principle whose introduction was considered a “drastic” measure by Dirac.¹ The fact that quantum superpositions do not exist in the macroscopic world hinders our intuition and leads to the apparently weird behaviour dictated by quantum mechanics. A famous example of this was posed by Schrödinger in 1935² who pointed out that quantum mechanics would predict bizarre situations such as a cat being simultaneously dead and alive. The existence of superpositions prescribed by quantum mechanics is valid for systems that are closed, that is, free from external influences. In contrast, real systems always couple to these external influences, the environment, which is typically composed of an extremely large number of degrees of freedom. Lack of knowledge about the environment is expressed by averaging (mathematically tracing) over the possible states of the environment degrees of freedom. This leads to an evolution of the density matrix of the system, in which the quantum superpositions are continuously reduced to classical probability distributions, a process generally known as decoherence. See for example, Refs. 3–5. One approach to describe decoherence is to treat the environment as a reservoir of quantum oscillators, each of which interacts with the quantum system in question. An example of such a reservoir-system interaction is the ensemble of empty electromagnetic field modes, each represented by a quantized harmonic oscillator, interacting with an atom so as to induce spontaneous emission. As a quantum superposition is made larger, decoherence tends to act more quickly. For truly macroscopic superpositions, such as Schrödinger's cat, decoherence occurs on such a short time scale that it is all but impossible to observe quantum coherences. However, mesoscopic systems present the possibility of studying, in a controlled way, the process of decoherence and the transition from quantum to classical behaviour.

In the past few years, techniques have been realized to generate mesoscopic superpositions, also called

Schrödinger cats, of motional states of trapped ions⁶ and of photon states in the context of cavity QED,⁷ where decoherence through coupling to ambient reservoirs and the sensitivity of the rate of decoherence on the size of cat were observed. In this work we extend the investigations beyond the ambient reservoirs and “engineer” the state of the reservoir, as well as the form of the system-reservoir coupling. One way this can be achieved for a system of trapped ions is by applying noisy potentials to the trap electrodes, simulating a hot resistor (reservoir) connected to the trap electrodes, with controllable temperature and spectrum. For a range of two-component superposition states, we demonstrate the expected exponential dependence of the decoherence rate on the separation of the components in Hilbert space. We also present the first study of decoherence into an engineered *quantum* reservoir, using laser cooling techniques to generate an effectively zero-temperature bath.^{8,9}

I. THEORETICAL PREDICTIONS

Decoherence of specific mesoscopic quantum superpositions, with a variety of couplings to a reservoir, has been investigated extensively in theory.^{3–5,8,10–12} The model in these studies is a system harmonic oscillator coupled to a bath of environment quantum oscillators. (These and other sources of decoherence in the context of trapped-ion experiments have been more recently discussed theoretically in Refs. 13–16.) As an illustration, consider the system oscillator to be in a superposition of coherent states. A coherent state¹⁷ of a harmonic oscillator is a Gaussian wavepacket which oscillates back and forth while retaining its shape. Quantum mechanically, a coherent state is represented by a state vector $|\alpha\rangle$, where $\alpha = |\alpha|e^{i\theta}$ is a complex number whose magnitude $|\alpha|$ is a dimensionless amplitude of the wavepacket's motion and whose phase θ is the phase of the oscillation at some initial time $t = 0$ (the phases of all subsequent coherent

ent manipulations are set relative to this initial phase). Coherent states are analogous to classical trajectories of a harmonic oscillator, approximated by a marble rolling back and forth in a bowl. A superposition of coherent states, $|\psi\rangle = N(|\alpha_1\rangle + |\alpha_2\rangle)$ (N is a normalization factor), can be visualized as a marble rolling in a superposition of two trajectories.

We consider the system oscillator to couple to the reservoir through an interaction proportional to the product of the amplitude of motion of the system oscillator and the amplitude of fluctuations of the reservoir. For brevity, we call this an *amplitude reservoir*. In the classical analogy, a hot amplitude reservoir behaves as if the bowl is subject to random displacements of its center, resulting in a random force on the marble. For a superposition of coherent states coupled to such a reservoir, a simple scaling law may be stated: the rate of decoherence (here a dephasing between the $|\alpha_1\rangle$ and $|\alpha_2\rangle$ components of $|\psi\rangle$) scales as the square of the separation of the wave packets, $|\alpha_1 - \alpha_2|^2$. In an idealized case where (a) the superposition is created, (b) the amplitude reservoir is coupled to the system for a time t , and then (c) the coupling is turned off, the remaining coherence between the two wave packets is⁴

$$C(t) = \exp \left[-|\alpha_1 - \alpha_2|^2 \xi t \right], \quad (1)$$

where ξ is a coupling constant between the reservoir and the system. The larger the size ($|\alpha_1 - \alpha_2|$) of the superposition, the faster the decoherence.

Another interesting basis of quantum states for the harmonic oscillator is the energy eigenstates, also known as Fock or number states. The Fock state $|n\rangle$ has energy $\hbar\omega(n+1/2)$ and represents a state of n units of quantized vibration, where $n \geq 0$ is an integer. Fock states have no classical analog, as they are delocalized in position and uniformly distributed in phase. A superposition of two Fock states $|\psi\rangle = (|n_1\rangle + |n_2\rangle)/\sqrt{2}$ loses coherence when the modes of the reservoir couple linearly to the energy of the oscillator, which is equivalent to averaging over a Gaussian distribution of phase shifts of the oscillator. We denote this case as a *phase reservoir*. The coherence between the two Fock states decays at a rate that scales as the square of the difference between the Fock indices, $|n_1 - n_2|^2$ given by⁴

$$C(t) = \exp \left[-|n_1 - n_2|^2 \kappa t \right], \quad (2)$$

where κ is a coupling constant.

II. TRAPPED IONS

In the experiments described here, a linear Paul trap, similar to the one described in Ref. 18, confines single $^9\text{Be}^+$ atomic ions in a harmonic potential, for which we isolate the axial motion at frequency $\omega = 2\pi \times$

11.3 MHz. Within the ion's electronic ground-state hyperfine manifold we restrict our attention to two states, the $|F=2, m_F=-2\rangle$ state, which we label $|\downarrow\rangle$, and the $|F=1, m_F=-1\rangle$ state, which we label $|\uparrow\rangle$, separated in energy by $\hbar\omega_0$, where $\omega_0 \approx 2\pi \times 1.25$ GHz and where F and m_F are the quantum numbers associated with the total angular momentum of the atomic state. The ion is cooled to the $n=0$ ground state of motion, denoted $|0\rangle$, and optically pumped to the $|\downarrow\rangle$ state with resolved-sideband stimulated Raman cooling.¹⁹ Thus, the initial state for all the experiments is $|\downarrow\rangle|0\rangle$.

We drive coherent stimulated Raman transitions with a pair of laser beams detuned approximately 12 GHz from the atomic resonance near 958 THz ($\lambda = 313$ nm). We employ three types of Raman transitions: (i) Copropagating beams with a difference frequency ω_0 between the two laser beams drive motion-independent spin-flip transitions, $|\downarrow\rangle|n\rangle \leftrightarrow |\uparrow\rangle|n\rangle$; (ii) To couple to the motion, we orient the laser beams so that their wavevector difference points along the trap axis. By driving the motional sidebands of the Raman spectrum^{13,20} at difference frequencies $\omega_0 + \omega\Delta n$, we coherently drive transitions between the states $|\downarrow\rangle|n\rangle$ and $|\uparrow\rangle|n + \Delta n\rangle$. (iii) The third type of Raman transition, with difference frequency ω and beams oriented as in (ii), approximates the harmonic-oscillator displacement operator $\mathcal{D}(\alpha)$, where the operator is defined^{4,5} by the relation $\mathcal{D}(\alpha)|0\rangle = |\alpha\rangle$. The displacement $|\alpha|$ is proportional to the duration of the laser pulse, and θ is set by the phase of the applied laser field.^{13,6} We can efficiently detect the $|\downarrow\rangle$ internal state of the ion by applying circularly polarized laser light resonant with the transition $|\downarrow\rangle \leftrightarrow |e\rangle$, where $|e\rangle$ is a short-lived excited electronic state that predominantly decays back to $|\downarrow\rangle$ by emitting a photon.¹⁹ In contrast, the transition $|\uparrow\rangle \leftrightarrow |e\rangle$ is out of resonance, and an ion in the state $|\uparrow\rangle$ scatters negligible light.

III. HIGH-TEMPERATURE AMPLITUDE RESERVOIR

The motion of a trapped ion couples to uniform electric fields \mathbf{E} through the potential $U = -q\mathbf{x} \cdot \mathbf{E}$, where \mathbf{x} is the displacement of the ion from its equilibrium position (proportional to the amplitude of motion) and q is the charge of the ion. This coupling is independent of the ion's internal state. Our engineered amplitude reservoir consists of random uniform electric fields applied along the axis of the trap, oscillating near the ion's axial-motion frequency ω . We generate axial fields in the trap by applying voltages to one of the trap electrodes. A commercial function generator produces pseudo-random voltages which are applied through a band-pass filter centered near ω , defining the frequency spectrum of the reservoir.

In all the experiments reported here, we measure the coherence of the quantum superpositions with single-atom interferometry, analogous to that used in our previous work.⁶ For example, to observe the effects of the

amplitude reservoir, the motional state of the ion is split into a superposition of two components, each associated with a different internal state of the ion, forming a Schrödinger-cat-like state.⁶ The superposition is then coupled to the reservoir, and finally the perturbed superposition is recombined by reversing the steps which initially created it. Repeating the experiment many times, the internal state of the ion is measured as a function of the relative phase of the creation and reversal steps, and the contrast of the resulting interference fringes characterizes the amount of coherence remaining after coupling to the reservoir.

In more detail, we first form a cat state of the form

$$|\psi_c\rangle = (|\downarrow\rangle|\alpha_\downarrow\rangle + |\uparrow\rangle|\alpha_\uparrow\rangle)/\sqrt{2}. \quad (3)$$

This is created by driving a Raman transition (type (i)) to generate an equal spin superposition, $|\downarrow\rangle|0\rangle \rightarrow (|\downarrow\rangle + |\uparrow\rangle)|0\rangle/\sqrt{2}$, followed by a pulse driving Raman transition (type (iii)), with laser polarizations such that $\alpha_\uparrow = -\alpha_\downarrow/2$ in Eq. 3.

A uniform electric field oscillating near the trap frequency ω (applied in the experiment for 3 μ s) results in the displacement operator $\mathcal{D}(\beta)$ acting equally on both $|\downarrow\rangle$ and $|\uparrow\rangle$, giving

$$|\psi_c\rangle \rightarrow |\psi'_c\rangle = (|\downarrow\rangle|\beta + \alpha_\downarrow\rangle + e^{i\phi_m}|\uparrow\rangle|\beta + \alpha_\uparrow\rangle)/\sqrt{2}, \quad (4)$$

where $\phi_m = \text{Im}\beta\Delta\alpha^*$ and $\Delta\alpha = \alpha_\downarrow - \alpha_\uparrow$. We probe the coherence by reversing the steps taken to generate the cat state. We first reverse the pulse on Raman transition (iii), resulting in the state

$$|\psi'_c\rangle \rightarrow |\psi''\rangle = (|\downarrow\rangle + e^{2i\phi_m}|\uparrow\rangle)|\beta\rangle/\sqrt{2}. \quad (5)$$

A final pulse on the motion-independent spin-flip transition (i), with phase δ relative to the first pulse on transition (i), leads to interference fringes with a residual phase shift $2\phi_m$. Averaging over the Gaussian random variable β , the probability to find the ion in the $|\downarrow\rangle$ state is²¹

$$P_\downarrow = \frac{1}{2} \left(1 - e^{-2|\Delta\alpha|^2\sigma^2} \cos \delta \right). \quad (6)$$

Interference fringes are generated by recording P_\downarrow while sweeping δ . The variance σ^2 of β is proportional to the mean-squared voltage noise $\langle V^2 \rangle$ (proportional to the temperature of the simulated resistor). A plot of the interference fringe contrast as a function of the applied mean-squared voltage, scaled by the squared “size” of the cat state $|\Delta\alpha|^2$, is shown in Fig. 1. Decay curves were recorded for a variety of superposition sizes $|\Delta\alpha|$, and all the data agree with a single exponential.

In addition to the engineered reservoir of the applied voltage noise, the ion also interacts with ambient fluctuating electric fields, which we expect to have the character of an amplitude reservoir. To examine this “natural” decoherence, we ran the experiment outlined above

without any applied voltage noise, and with a variable time t between the creation of the cat state and the recombination. The fringe visibility as a function of $|\Delta\alpha|^2 t$ is shown in the inset to Fig. 1. The decay curves are normalized to unity at $t = 0$. The decay of the fringe visibility is exponential, and the decay constant $\gamma \simeq 6.7 \times 10^{-3}/\mu\text{s}$ is consistent with the measured heating rate¹³ of $\gamma \simeq 5.9 \times 10^{-3}/\mu\text{s}$ for this apparatus. The effects of this ambient reservoir were negligible during the time (3 μ s) that the engineered amplitude reservoir was coupled to the ion.

IV. HIGH-TEMPERATURE PHASE RESERVOIR

A phase reservoir coupled to the ion is simulated by random variations in the trap frequency ω , changing the phase of the ion oscillation without changing its energy. We realize this coupling experimentally by modulating the trap frequency. A random voltage noise source is passed through a low-pass filter network with a cut-off frequency well below ω to maintain adiabaticity. The fluctuations in potential are applied symmetrically to the trap electrodes so as to produce quadratic field gradients and negligible uniform fields. This in turn perturbs the trap frequency, by $\delta\omega(t)$. When integrated over the time (20 μ s) of the applied noise, the ion’s motion is phase-shifted by $\phi = \int \delta\omega dt$. This technique yields a Gaussian-distributed ensemble of phase shifts with variance σ^2 proportional to the applied mean-squared voltage noise $\langle V^2 \rangle$.

Motional decoherence caused by a phase reservoir is clearly illustrated with a superposition of two Fock states. We generate superpositions of Fock states of the form $|\psi\rangle = |s\rangle(|n\rangle + |n'\rangle)/\sqrt{2}$, where $s = \downarrow$ or \uparrow , with pulses on the Raman motional sidebands (case (ii) above) as in Ref. 20. The trap frequency is then perturbed by the applied random potentials, and the Fock states of the superposition acquire a relative phase factor $e^{i\phi\Delta n}$, where $\Delta n = n - n'$. The steps that created the superposition are then reversed, with a relative phase difference δ between the creation and reversal pulses, leading to a probability of detecting the ion in the $|\downarrow\rangle$ state,²¹

$$P_\downarrow = \frac{1}{2} \left[1 + e^{-|\Delta n|^2\sigma^2/2} \cos \delta \right]. \quad (7)$$

Interference fringes are recorded by varying δ as in the Schrödinger cat interferometer. The fringe contrast is plotted as a function of $|\Delta n|^2\langle V^2 \rangle$ in Fig. 2. As with the Schrödinger cat states and amplitude reservoir, the data were fitted by an exponential in $|\Delta n|^2\langle V^2 \rangle$.

V. ZERO-TEMPERATURE RESERVOIR

A third type of engineered reservoir requires a quantum mechanical description. This reservoir is a bath of laser cooling light plus optical spontaneous emission, an engineered (nearly) zero-temperature reservoir following the suggestion of Poyatos, Cirac, and Zoller.⁸ Our implementation, shown in Fig. 3, is essentially a continuous Raman cooling technique. A pair of Raman beams (case ii) tuned to the first red sideband couple the states $|\downarrow\rangle|n\rangle \leftrightarrow |\uparrow\rangle|n-1\rangle$. Concurrently, an optical pumping beam causes spontaneous-Raman transitions from $|\uparrow\rangle$ to $|\downarrow\rangle$ through an unstable excited state $|e\rangle$, which decays at rate Γ . The Raman coupling strength is characterized by the Rabi frequency Ω_{rsb} , a function of the intensity and detuning of the Raman beams.¹³ If the Rabi frequency of the optical pumping beam is Ω_p , then we can define an effective damping rate for the $|\uparrow\rangle$ state of $\gamma = \Omega_p^2/\Gamma$, valid for our case of $\Omega_p \ll \Gamma$. From the diagram in Fig. 3 we see that all populations are driven towards the state $|\downarrow\rangle|0\rangle$, the defining property of a zero-temperature reservoir. By varying the strength of the Raman and optical pumping couplings, we have control over the reservoir parameters.

In the experiment, we examine the time evolution of the coherence of the Fock state superposition $\psi = |\downarrow\rangle(|0\rangle + |2\rangle)/\sqrt{2}$ for varying lengths of reservoir interaction time. The interferometry is the same as in the study of the phase reservoir, where the Fock superposition is created, coupled to the reservoir, recombined, and probed, generating interference fringes. The data are shown in Fig. 4. Each data point is the contrast of the fringes after the system interacts with the reservoir. We show two cases, $\gamma < \Omega_{\text{rsb}}$ and $\gamma > \Omega_{\text{rsb}}$. In the former case, the coherence between the $|0\rangle$ and $|2\rangle$ state disappears and reappears over time, with an overall decay of the fringe contrast. The underlying effect is population transfer back and forth (Rabi flopping) between the states $|\downarrow\rangle|2\rangle$ and $|\uparrow\rangle|1\rangle$ with a coupling of the $|\uparrow\rangle|1\rangle$ state to the outside environment through spontaneous Raman scattering. In effect, we have restricted the size of the environment (here the manifold of $|\uparrow\rangle|n\rangle$ states, weakly coupled to the outside environment) to an extent where we can reverse the effects of decoherence (of the $\psi = |\downarrow\rangle(|0\rangle + |2\rangle)/\sqrt{2}$ state) in a way similar to that proposed by Raimond, *et al.*²² This is also a striking example of non-exponential decay²³ in a context being investigated by Thompson, *et al.*²⁴ For the case $\gamma > \Omega_{\text{rsb}}$, the fringe contrast decreases monotonically to zero. Even in the case of monotonic decay, a deviation from exponential is observed, a manifestation of the quantum Zeno effect.^{24, 25}

Although the $\gamma < \Omega_{\text{rsb}}$ data illustrate how coherence transferred to the environment can be recovered, an alternative explanation would say that by transferring the $|\downarrow\rangle|2\rangle$ component of the superposition to the $|\uparrow\rangle|1\rangle$ state, we gain “which-path” information in our interferometer

- the paths being the $|\downarrow\rangle|0\rangle$ and $|\downarrow\rangle|2\rangle$ parts of the superposition. The oscillation in which-path information is analogous to that illustrated by the experiments of Chapman, *et al.*²⁶ and Dürr, *et al.*²⁷

VI. CONCLUSIONS

The decoherence caused by the engineered high-temperature reservoirs described above can be explained by ensemble-averaging over random classical fields applied to the ion.^{21, 28} From previous experiments,²⁰ we know that we can undo the effects of this decoherence by applying, in each experiment, a pulse of radiation that reverses the “random” displacement. Similarly, the experiments here could also be carried out by coupling a hot resistor (with appropriate spectral filtering) between the trap electrodes (our case would correspond to a limit where the temperature $T \rightarrow \infty$ and the damping resistance $R \rightarrow 0$).¹⁰ However, even in this case we could, subject to both practical and fundamental measurement uncertainties, record the voltages applied to the electrodes and reverse the effects of the random noise in each experiment. If we choose to ignore any knowledge of the electrical potentials applied to the trap electrodes, we can account for the observations just as well by considering the ion to be coupled to a large number of quantum oscillators, forming a heat bath. In the latter case, the state of the ion is entangled with that of the environment oscillators. After tracing over the environment variables, we are left with a reduced system, involving only the ion. The behavior is the same as that obtained in the former case, in which the decoherence is caused by a deliberately applied external potential, but the environment is not considered to be a dynamical system itself.^{3, 4} Loosely speaking, the effect of an environment oscillator in the latter case is replaced by that of a single Fourier component of the electrical potential in the former case. Therefore, in the high-temperature limit simulated by the first two experiments, one need not consider the entanglement with the environment since the environment noise can be sensed (classically) and its effects reversed. This is to be contrasted with the decay into a zero-temperature reservoir as in cavity-QED experiments⁷ or in the experiments described in the previous section, where, after the quantum system couples to the environment through spontaneous emission, a measurement of the environment is not sufficient to reverse the effects of decoherence.

The methods to engineer reservoirs presented here begin to broaden the field of experimental investigations of decoherence. With control over the reservoir parameters combined with non-classical motional states of trapped ions, detailed comparisons between theory and experiment are possible. Here we have simulated the decoherence caused by coupling a charged atom to a hot resistor (reservoir) by applying noisy voltages to the ion trap electrodes. The cases considered demonstrate

a quadratic dependence of the rate of decoherence on the size of the superpositions, demonstrating the difficulty in generating truly macroscopic superpositions, such as Schrödinger's cat. As a practical matter, these "high-temperature" sources of noise are important because they currently limit the performance of a trapped-ion quantum computer.¹³ We have also simulated a zero-temperature reservoir by using laser cooling to damp the ion motion. Extensions of the technique used to generate this zero-temperature bath should permit some interesting system-bath interactions that would be difficult to realize in any other way. One intriguing possibility is generating a squeezed reservoir, where all initial states asymptotically relax to a squeezed state of motion.⁸ Other couplings can be tailored to relax the system into a Schrödinger-cat state.^{29,30}

* Work of the US government. Not subject to US copyright.

- [1] Dirac, P. A. M., 1958, *The Principles of Quantum Mechanics*, (Oxford Univ. Press, Clarendon) p. 4.
- [2] Schrödinger, E., Die gegenwärtige situation in der quantenmechanik, 1935, *Naturwissenschaften* **23**, 807-812, 823-828, 844-849.
- [3] Zurek, W. H., Decoherence and the transition from quantum to classical, 1991, *Physics Today*, **44** (Oct.), 36-44.
- [4] Walls, D. F., and Milburn, G. J., 1994, *Quantum Optics*, (Springer-Verlag, Berlin).
- [5] Bužek, V., and Knight, P. L., Quantum interference, superposition states of light, and nonclassical effects, 1995, *Progress in Optics* **XXXIV**, 1-158.
- [6] Monroe, C., Meekhof, D. M., King, B. E., and Wineland, D. J., A "Schrödinger cat" superposition state of an atom, 1996, *Science* **272**, 1131-1136.
- [7] Brune, M., Hagley, E., Dreyer, J., Maître, X., Maali, A., Wunderlich, C., Raimond, J. M., and Haroche, S., Observing the progressive decoherence of the "meter" in a quantum measurement, 1996, *Phys. Rev. Lett.* **77**, 4887-4890.
- [8] Poyatos, J. F., Cirac, J. I., and Zoller, P., Quantum reservoir engineering with laser cooled trapped ions, 1996, *Phys. Rev. Lett.* **77**, 4728-4731.
- [9] Marzoli, I., Cirac, J. I., Blatt, R., and Zoller, P., Laser cooling of trapped three-level ions: designing two-level systems for sideband cooling, 1994, *Phys. Rev. A* **49**, 2771-2779.
- [10] Caldeira, A. O., and Leggett, A. J., Influence of damping on quantum interference: an exactly soluble model, 1985, *Phys. Rev. A* **31**, 1059-1066.
- [11] Walls, D. F., and Milburn, G. J., Effect of dissipation on quantum coherence, 1985, *Phys. Rev. A* **31**, 2403-2408.
- [12] Collett, M. J., Exact density-matrix calculations for simple open systems, 1988, *Phys. Rev. A* **38**, 2233-2247.
- [13] Wineland, D. J., Monroe, C., Itano, W. M., Leibfried, D., King, B. E., and Meekhof, D. M., Experimental issues in coherent quantum-state manipulation of trapped atomic ions, 1998, *J. Res. NIST* **103**, 259-328.
- [14] Schneider, S., and Milburn, G. J., Decoherence in ion traps due to laser intensity and phase fluctuations, 1998, *Phys. Rev. A* **57**, 3748-3752.
- [15] Murao, M. and Knight, P. L., Decoherence in nonclassical motional states of a trapped ion, 1998, *Phys. Rev. A* **58**, 663-669.
- [16] Schneider, S., and Milburn, G. J., Decoherence and fidelity in ion traps with fluctuating trap parameters, 1999, *Phys. Rev. A* **59**, 3766-3774.
- [17] Glauber, R. J., Coherent and incoherent states of the radiation field, 1963, *Phys. Rev.* **131**, 2766-2788.
- [18] Raizen, M. G., Gilligan, J. M., Bergquist, J. C., Itano, W. M., and Wineland, D. J., Ionic crystals in a linear Paul trap, 1992, *Phys. Rev. A* **45**, 6493-6501.
- [19] Monroe, C., Meekhof, D. M., King, B. E., Jefferts, S. R., Itano, W. M., Wineland, D. J. and Gould, P., Resolved-sideband Raman cooling of a bound atom to the 3D zero-point energy, 1995, *Phys. Rev. Lett.* **75**, 4011-4014.
- [20] Meekhof, D. M., Monroe, C., King, B. E., Itano, W. M., and Wineland, D. J., Generation of nonclassical motional states of a trapped atom, 1996, *Phys. Rev. Lett.* **76**, 1796-1799.
- [21] Myatt, C. J., King, B. E., Turchette, Q. A., Sackett, C. A., Kielpinski, D., Itano, W. M., Monroe, C., and Wineland, D. J., Decay of quantum superpositions into engineered reservoirs, 1999, in *Laser Spectroscopy 13*, ed. by R. Blatt, J. Eschner, D. Leibfried, F. Schmidt-Kaler (World Scientific, Singapore), in press.
- [22] Raimond, J. M., Brune, M., and Haroche, S., Reversible decoherence of a mesoscopic superposition of field states, 1997, *Phys. Rev. Lett.* **79**, 1964-1967.
- [23] Wilkinson, S. R., Bharucha, C. F., Fisher, M. C., Madison, K. W., Morrow, P. R., Niu, Q., Sundaram, B., and Raizen, M. G., Experimental evidence for non-exponential decay in quantum tunnelling, 1997, *Nature* **387**, 575-577.
- [24] Thompson, R. C., Hernandez-Pozos, J. -L., Höffges, J., Segal, D. M., and Vincent, J. R., The quantum Zeno effect in trapped ions, 1999, in *Trapped Charged Particles and Fundamental Physics*, edited by D.H.E. Dubin and D. Schneider, AIP Conf. Proc. 457 (AIP Press, Woodbury, NY), 388-392.
- [25] Itano, W. M., Heinzen, D. J., Bollinger, J. J., and Wineland, D. J., Quantum Zeno effect, 1990, *Phys. Rev. A* **41**, 2295-2300.
- [26] Chapman, M. S., Hammond, T. D., Lenef, A., Schmiedmayer, J., Rubenstein, R. A., Smith, E., and Pritchard, D. E., Photon Scattering from atoms in an interferometer: coherence lost and regained, 1995, *Phys. Rev. Lett.* **75**, 3783-3787.
- [27] Dürr, S., Nonn, T., and Rempe, G., Fringe visibility and which-way information in an atom interferometer, 1998, *Phys. Rev. Lett.* **81**, 5705-5709.
- [28] Itano, W. M., Monroe, C., Meekhof, D. M., Leibfried, D., King, B. E., and Wineland, D. J., Quantum harmonic oscillator state synthesis and analysis, 1997, *SPIE Proc.* **2995**, 43-55.
- [29] de Matos Filho, R. L., and Vogel, W., Even and odd

coherent states of the motion of a trapped ion, 1996, *Phys. Rev. Lett.* **76**, 608-611.

- [30] Garraway, B. M., Knight, P. L., and Plenio, M. B., Generation and preservation of coherence in dissipative quantum optical environments, 1998 *Physica Scripta* **T76**, 152-158.

VII. ACKNOWLEDGMENTS

We thank the U.S. National Security Agency, Army Research Office, and Office of Naval Research for support. We thank P. Zoller, H. Mabuchi, and W. Zurek for helpful discussions. We thank them, D. Leibfried, M. Rowe, D. Sullivan, and M. Lombardi for comments on the manuscript.

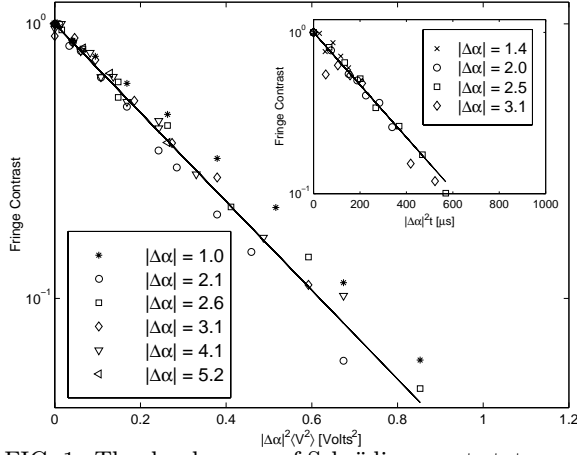


FIG. 1. The decoherence of Schrödinger-cat states coupled to an amplitude reservoir. In the main figure, each point is the measured contrast of the interference fringes after noisy potentials were applied to the trap electrodes. The contrast at $\langle V^2 \rangle = 0$ is scaled to unity in order to make comparisons between different values of $|\Delta\alpha|$. The size of the superposition, $|\Delta\alpha|$, varies linearly with the pulse time for Raman transition type (iii). The applied mean-squared voltage $\langle V^2 \rangle$ is scaled by $|\Delta\alpha|^2$. The solid line is a fit to an exponential. In the inset, fringe contrast vs. time of interaction with ambient fields is plotted. Again, the fringe contrast is scaled to unity at $t = 0$ for comparison between different values $|\Delta\alpha|$. The solid line is a fit to an exponential.

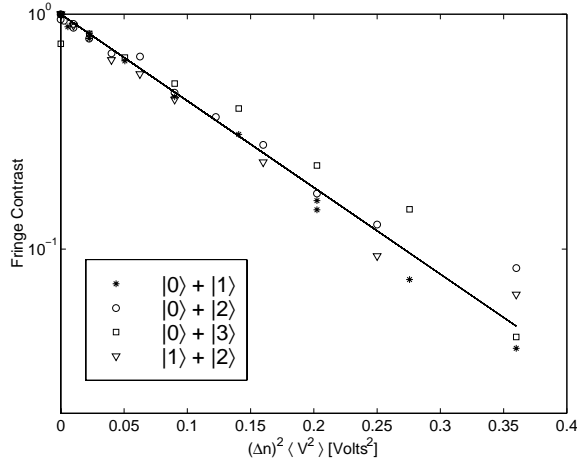


FIG. 2. Decoherence of superpositions of Fock states coupled to the phase reservoir. The data points are the measured fringe contrast. The fringe contrast is normalized to unity at $\langle V^2 \rangle = 0$. The mean squared voltage applied to the trap electrodes is scaled by the squared size of the superposition $|\Delta n|^2$. The solid line is a fit to an exponential.

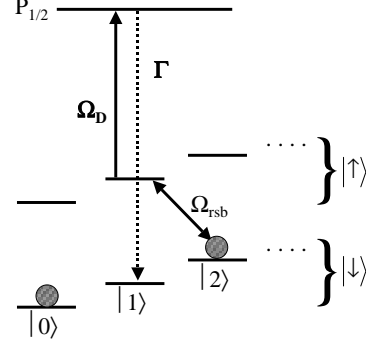


FIG. 3. Implementation of an engineered zero-temperature reservoir. The states $|\downarrow\rangle|n\rangle$ and $|\uparrow\rangle|n-1\rangle$ are coupled by driving the red-Raman motion-sensitive transition, case (ii) in the text. The state $|\uparrow\rangle$ is coupled to the environment by applying a weak optical pumping beam. The circles represent the superposition generated before applying this zero-temperature reservoir. The arrows show how the population in the $|\downarrow\rangle|2\rangle$ state is driven to the $|\uparrow\rangle|1\rangle$ state, and subsequently to the $|\downarrow\rangle|1\rangle$ state through spontaneous Raman scattering.

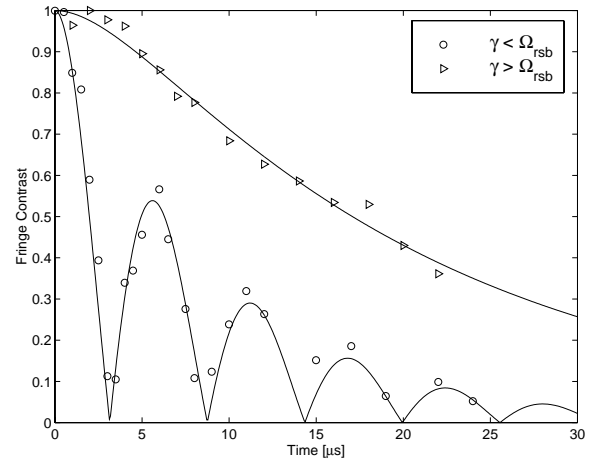


FIG. 4. Decoherence of a Fock state superposition into the engineered zero-temperature reservoir. Fringe contrast is plotted as a function of the time the system is coupled to the zero temperature reservoir. The only difference in the two cases shown was the intensity of the optical pumping beam (see Fig. 3).